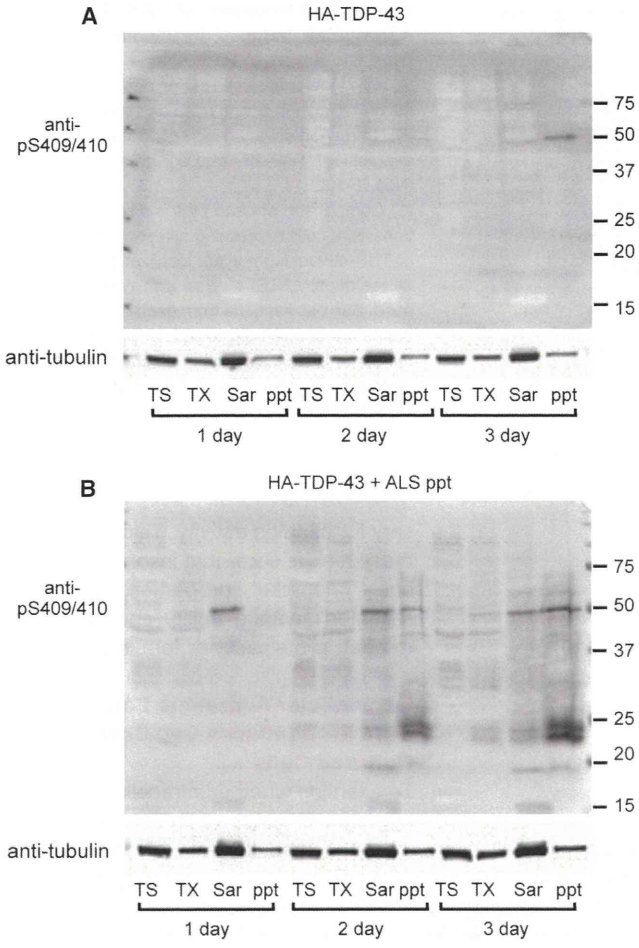

Figure 2. Time Course of Production of TDP-43 CTFs

(A and B) Cells transiently expressing HA-TDP-43 plasmid treated without (A) or with (B) ALS ppt were incubated for 1–3 days and then harvested. Proteins were differentially extracted and subjected to immunoblot analyses. Blots were probed with anti-pS409/410.

plasmid and ALS ppt, surprisingly, full-length HA-TDP-43 was accumulated even on day 1, whereas CTFs were not detected in any fraction at this time (Figure 2B). On and after day 2, not only full-length HA-TDP-43 but also CTFs were aggregated in cells. Thus, intracellular aggregation of full-length TDP-43 precedes generation of TDP-43 CTFs, suggesting that production of CTFs is not essential for formation of intracellular TDP-43 aggregates.

Characteristic CTFs of Insoluble TDP-43 in Each Disease Type Were Reproduced in a Self-Templating Manner in Cultured Cells

TDP-43 proteinopathy is classified into four types based on the predominant TDP-43-positive structures: type A mainly includes FTLD-TDP with GRN mutations, type B contains ALS and FTLD-MND, type C is representative of sporadic FTLD-TDP showing impairment of semantic memory, and type D refers to the pathology associated with inclusion body myopathy with early-onset Paget's disease and frontotemporal dementia caused by *VCP* mutations (Mackenzie et al., 2011). Each type is also characterized biochemically by the patterns of insoluble TDP-43 CTFs detected with anti-pS409/410 (Hasegawa et al., 2008; Tsuji et al., 2012). We prepared Sar-ppt from several types of brains (Figure 3A) and introduced them as seeds into cells expressing a plasmid encoding TDP-43. After 3 days of incubation, cells were harvested and each Sar-ppt was analyzed by immunoblotting with anti-pS409/410. In Figures 3A and 3B, all seeds prepared from TDP-43 proteinopathy brains (Nos. 1–8), but not from DLB (No. 9) or Pick's disease (No. 10) brain, were shown to function as seeds for TDP-43 aggregation in cultured cells, but the seeding efficiencies were different: type A and B seeds were more effective than type C. No sample was available from FTLD-TDP type D brain.

Next, to check whether each characteristic deposit of CTF was reproduced in cultured cells in the presence of each type of seed, we prepared insoluble fractions from TDP-43-expressing cells treated with seeds from each type of brain, and analyzed them by immunoblotting using anti-pS409/410. Interestingly, the band patterns of CTFs in the insoluble fraction (ppt) of cells expressing TDP-43 in the presence of each type of seed were different from each other, but quite similar to that of insoluble TDP-43 prepared as seeds from the corresponding patients (type A, B, or C), indicating that plasmid-derived TDP-43 is aggregated in a template-dependent manner in the presence of each type of seed (Figure 3C). These results suggest that seed-dependent TDP-43 aggregation, like prion aggregation, occurs in a self-templating manner. Insoluble TDP-43 from diseased brains appears to have features similar to those of pathogenic prion.

Insoluble TDP-43 Has Prion-like Properties

Next, we examined whether insoluble TDP-43 from brains of patients has prion-like characteristics. First, we tested whether detergent-insoluble TDP-43 prepared from cells containing TDP-43 aggregates as well as seeds from brains can promote intracellular TDP-43 aggregation. Triton X-100 (TX)-insoluble fraction was prepared as seeds from cells containing aggregates (Figure 4A, right panel) and introduced into cells. In a control experiment, we confirmed that insoluble seeds from cells expressing HA-TDP-43 treated with ALS ppt (HA-TDP-43+ALS ppt) did not serve efficiently as seeds for endogenous TDP-43 aggregation (Figure S3A). In cells expressing HA-TDP-43 and treated with TX-insoluble seeds from cells transfected with both HA-TDP-43 and ALS ppt, phosphorylated full-length HA-TDP-43 and CTFs were observed in the insoluble fraction (ppt; Figure 4A), whereas the band of phosphorylated full-length HA-TDP was hardly detectable in the insoluble fraction from cells expressing HA-TDP-43 and treated with TX-insoluble seed from cells without transfection (none) or treated with TX-insoluble seed from cells expressing HA-TDP-43 alone (HA-TDP-43). In immunocytochemical analyses of cells expressing HA-TDP-43 and treated with TX-insoluble seeds from cells transfected with both HA-TDP-43 and ALS ppt (HA-TDP-43+ALS ppt), we observed inclusions positive for both anti-pS409/410 and anti-Ub (Figure 4B), which were very similar to those observed in cells expressing

Cell PRESS
Open ACCESS

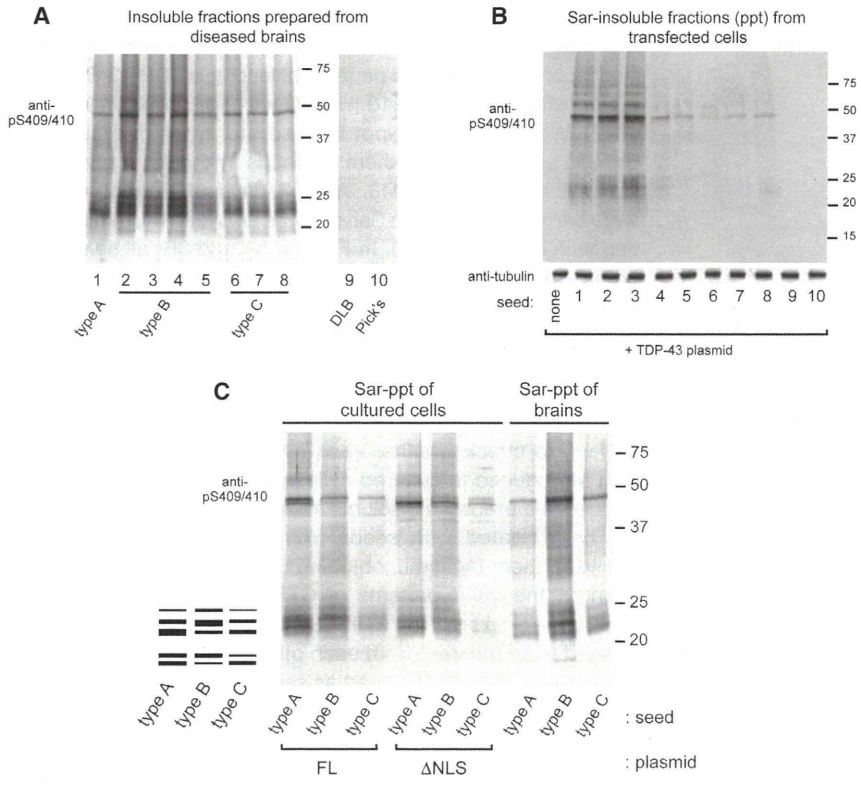

Figure 3. Formation of Self-Templating Aggregates Induced by Insoluble TDP-43 from the Brains of Patients

(A) Immunoblot analyses of Sar-ppt prepared from several diseased brains used as seeds.

(B) Immunoblot analyses of Sar-ppt of cells expressing TDP-43 treated with each seed (Nos. 1–10).

(C) Comparison of band patterns of Sar-ppt fractions from cells expressing full-length TDP-43 (FL) or TDP-43 lacking nuclear localization signal (78–84 residues: ΔNLS) treated with type A, B, or C seed. Sar-ppt fractions from each of the diseased brains are shown next to cellular ppt fractions on the same blot. A schematic diagram of the band pattern of TDP-43 CTFs is also presented. Blots were probed using anti-pS409/410.

HA-TDP-43 treated with ALS ppt (Figure 1E). These results indicate that TX-insoluble seeds produced from cells containing TDP-43 aggregates can function as seeds for further aggregation of TDP-43.

We also checked the effects of heat treatment or proteinase digestion of insoluble TDP-43 on seeding ability. Each type of seed was treated or not treated at 100°C for 5 min (boiling) and analyzed by immunoblotting with anti-pS409/410. No marked differences in the band patterns of each type of seed were seen before or after the boiling treatment (Figure 4C, left panel). Then, these seeds were introduced into TDP-43-expressing cells, and Sar-ppts prepared from the cells were analyzed by immunoblotting with anti-pS409/410 (Figures 4C and S3B). In the case of type A seed, the seeding effect on TDP-43 aggregation was unaffected by boiling, whereas the ability of type B and C seeds to induce TDP-43 aggregation was almost abrogated after boiling (Figure 4C, middle and right panels). All of these seeds were easily degraded into <20 kDa CTFs by Proteinase K (ProK) treatment (Figure 4D, left panel). However, seeding ability to induce intracellular TDP-43 aggregation was retained even after ProK digestion (Figure 4D, middle and right panels, and Figure S3C).

Furthermore, we tested whether formic acid, which destroys the β-sheet structure of proteins, influences the seeding ability of insoluble TDP-43. As shown in Figures 4E, S3D, and S3E, insoluble fractions from type A, B, and C brains treated with formic acid did not induce intracellular TDP-43 aggregation, suggesting that β-sheet-rich structure is necessary for seeding activity. Taken together, these results show that insoluble TDP-43 has prion-like properties, including repeated seeding ability and sensitivity to heat, proteinase, or formic acid.

Intracellular Aggregate Formation of TDP-43 Induces Cell Death in Cultured Cells

To examine whether intracellular TDP-43 aggregates cause neuronal dysfunction leading to cell death, we measured the rate of cell death in cells containing intracellular TDP-43 aggregates by means of lactate dehydrogenase (LDH) assay. Cells transfected with TDP-43 were treated with insoluble fractions from TDP-43 proteinopathy brains or Pick's disease brain and incubated for 3 days, followed by LDH assay. As shown in Figure 5A, the rate of cell death was almost 5% in cells treated only with insoluble fractions from type B or plasmid transfection, whereas it was ~20% in cells expressing TDP-43 and treated with each TDP-43 proteinopathy brain extract. These cell lysates were also analyzed by immunoblotting. Increased cell death of these cells was accompanied by deposition of phosphorylated TDP-43 in the Sar-ppt fraction (Figure 5B). However, no significant cell death was observed in cells expressing TDP-43 and treated with Pick's disease brain extract, in which phosphorylated TDP-43 was not deposited. These results suggest that increased cell death of cells containing TDP-43 aggregates is correlated with the amount of intracellular TDP-43 aggregates.

Intracellular Accumulation of TDP-43 Aggregates Elicits Proteasome Dysfunction

Previously, we reported that proteasome activity was suppressed in cells containing intracellular α-synuclein aggregates (Nonaka et al., 2010). To examine whether intracellular aggregates of TDP-43 also induce proteasome dysfunction, we assayed proteasome activity in cells containing TDP-43 aggregates by using the GFP-CL1 reporter (Bence et al., 2001), which is available to monitor proteasome activity in cultured cells (Nonaka and Hasegawa, 2009; Nonaka et al., 2010).

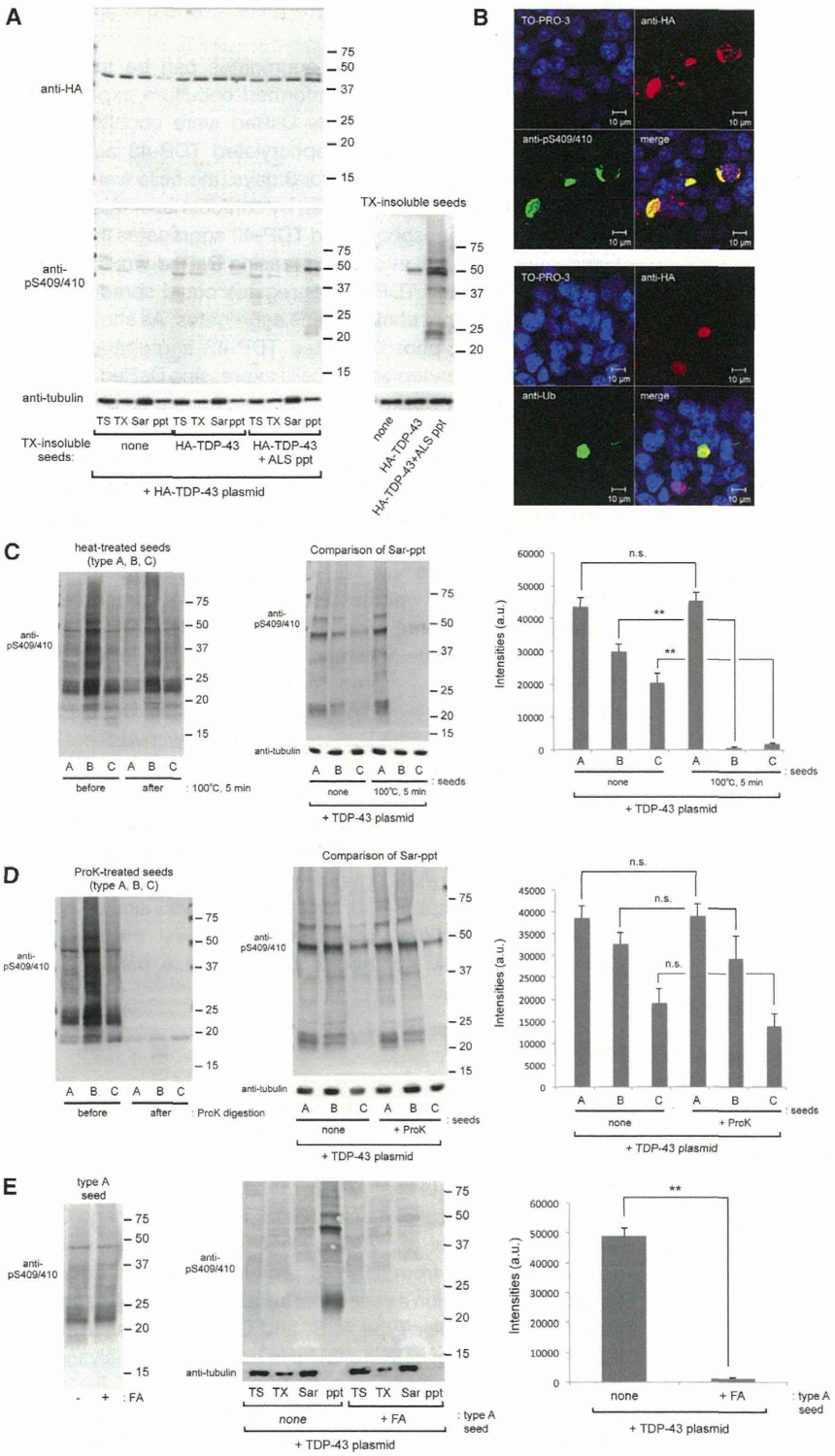

Figure 4. Characterization of the Prion-like Properties of Detergent-Insoluble TDP-43 from Brains

(A) Immunoblot analyses of cells expressing HA-TDP-43 and treated with Triton X-100-insoluble fractions (TX-insoluble seeds) prepared from the following cells, using anti-HA (upper) and anti-pS409/410 (lower): none, mock cells; HA-TDP-43, cells expressing HA-TDP-43; and HA-TDP-43+ALS ppt, cells expressing HA-TDP-43 and treated with ALS ppt. These TX-insoluble seeds (10 μg each) were also immunoblotted with anti-pS409/410 (lower right).

(B) Confocal laser microscopy analyses of cells expressing HA-TDP-43 and treated with TX-insoluble seed from cells transfected with both HA-TDP-43 and ALS ppt (HA-TDP-43+ALS ppt) immunostained with anti-HA (red), anti-pS409/410 (green), or anti-Ub (green), and counterstained with TO-PRO-3 (blue). Scale bars: 10 μm.

(C) Effect of heat treatment on the seeding ability of each type of seed. Each seed before and after heat treatment (100°C for 5 min) was analyzed by immunoblotting using anti-pS409/410 (left). Then, cells expressing TDP-43 were treated with these fractions as seeds. After 3 days of incubation, Sar-ppt fractions were prepared and analyzed by immunoblotting using anti-pS409/410 (middle). The immunoreactivity of each lane that was positive for anti-pS409/410 was quantified and the results are expressed as means + SEM (n = 3). **p < 0.0001 by Student's t test; n.s., not significant; a.u., arbitrary unit. See also Figure S3.

(D) Effect of ProK on the seeding ability of each type of seed. Each seed before and after ProK digestion (final 20 μg/mL ProK at 37°C for 30 min) was analyzed by immunoblotting using anti-pS409/410 (left). Then, cells expressing TDP-43 were treated with these fractions as seeds. After 3 days of incubation, the Sar-ppt fractions were analyzed by immunoblotting using anti-pS409/410 (middle). The immunoreactivity of each lane that was positive for anti-pS409/410 was quantified and the results are expressed as means + SEM (n = 3). n.s., not significant; a.u., arbitrary unit. See also Figure S3.

(E) Effect of formic acid (FA) on the seeding ability of type A seed. Type A seed with or without FA treatment was analyzed by immunoblotting using anti-pS409/410 (left). Then, cells expressing TDP-43 were treated with these fractions as seeds. After 3 days of incubation, fractionated samples were analyzed by immunoblotting using anti-pS409/410 (right). The immunoreactivity of ppt fractions that were positive for anti-pS409/410 was quantified and the results are expressed as means + SEM (n = 3). **p < 0.0001 by Student's t test. a.u., arbitrary unit. See also Figure S3.

Cells were transfected with TDP-43 and GFP-CL1 plasmids overnight, followed by transduction of ALS ppt. After 3 days of incubation, the cells were analyzed by confocal microscopy and immunoblotting. As shown in Figures 6A and 6B, GFP fluorescence in cells transfected with GFP-CL1 alone was very low due to degradation of GFP-CL1 by proteasome. When cells expressing GFP-CL1 were treated with proteasome inhibitor MG132 (0.1 μM), GFP fluorescence intensity

Cell PRESS
Open ACCESS

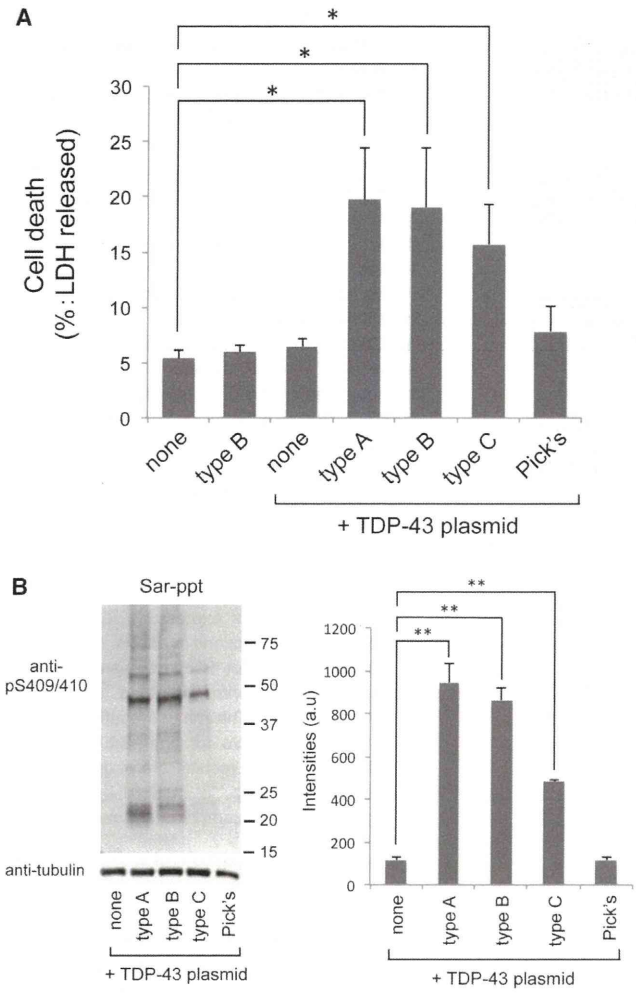

Figure 5. Cell Death Induced by the Formation of Intracellular TDP-43 Aggregates

(A) The extent of cell death of transfected cells was quantified by an LDH release assay. Cells treated with type B seed alone (type B), cells transfected with TDP-43 plasmid alone, or cells expressing TDP-43 and treated with Sar-ppt from type A, B, or C, or Pick's disease brains were cultured, and a cell death assay was performed 3 days thereafter. The results are expressed as means + SEM (n = 5). *$p < 0.05$ versus "none" by Student's t test.

(B) Immunoblot analyses of Sar-ppt from cells expressing TDP-43 and treated with extracts of type A, B, C, and Pick's disease brains, using anti-pS409/410. Immunoreactivity to anti-pS409/410 was quantified in each lane. The results are expressed as means + SEM (n = 3). **$p < 0.001$ versus "none" by Student's t test. a.u., arbitrary unit.

was significantly higher. GFP fluorescence in cells transfected with TDP-43 alone or treated with ALS ppt alone was as low as that in cells expressing only GFP-CL1, whereas it was significantly higher in cells expressing TDP-43 and treated with ALS ppt. We confirmed that cells containing phosphorylated TDP-43 aggregates were strongly positive for GFP (Figure 6C). These results suggest that proteasome activity is suppressed in cells harboring intracellular TDP-43 aggregates.

Phosphorylated TDP-43 Aggregates Are Propagated between Cultured Cells

To examine whether TDP-43 aggregates can be transferred between cultured cells, we performed coculture experiments. SH-SY5Y cells expressing only DsRed were cocultured with SH-S5Y5 cells harboring phosphorylated TDP-43 aggregates in a 1:1 ratio. After incubation for 3 days, the cells were stained with anti-pS409/410 and analyzed by confocal laser microscopy. The presence of phosphorylated TDP-43 aggregates immunolabeled with Alexa-488 in cells expressing DsRed would indicate that phosphorylated TDP-43 aggregates could spread to cells that originally did not contain these aggregates. As shown in Figures 7A and 7B, phosphorylated TDP-43 aggregates (green) were found in the cytoplasm of cells expressing DsRed. The percentage of DsRed-positive cells that also contained phosphorylated TDP-43 aggregates was calculated to be 2.9% ± 0.8%. In three-dimensional image modeling of a DsRed-expressing cell with TDP-43 aggregates, the signal of phosphorylated TDP-43 aggregates was merged with that of DsRed in the X-Z and Y-Z cross-sections (Figure 7B).

Next, we examined how TDP-43 aggregates are released from cells. It has been hypothesized that protein aggregates are released via exosome (Fevrier et al., 2004; Goedert et al., 2010). To investigate whether this mechanism operates for TDP-43 aggregates, we prepared exosome fractions from cells expressing TDP-43 plasmid alone, cells treated with ALS ppt alone, or cells expressing TDP-43 and treated with ALS ppt using the ExoQuick-TC kit (SBI). Immunoblot analyses showed that in cells expressing TDP-43 and treated with ALS ppt, the band intensity of full-length TDP-43 in the exosome fraction was significantly increased as compared with that in cells transfected with TDP-43 plasmid or ALS ppt alone (Figure 7C), whereas expression of the exosome marker protein CD63 was similar in all of the exosome fractions. These results suggest the possibility that exosome may contribute to the release of intracellular TDP-43 aggregates.

DISCUSSION

Prion-like propagation of aggregated proteins in neurodegenerative diseases is well established (Clavaguera et al., 2009; Desplats et al., 2009; Frost et al., 2009; Goedert et al., 2010; Kordower et al., 2008; Li et al., 2008; Luk et al., 2009; Nonaka et al., 2010; Masuda-Suzukake et al., 2013; Polymenidou and Cleveland, 2011; Ren et al., 2009). Here, we show that insoluble TDP-43 prepared from TDP-43 proteinopathy brains (type A, B, and C) can function as seeds for intracellular TDP-43 aggregation in cultured cells. Type A, B, and C brains showed distinct banding patterns of TDP-43 CTFs in immunoblot analyses with anti-pS409/410 (Hasegawa et al., 2008; Tsuji et al., 2012). The band patterns of characteristic CTFs are thought to reflect structural differences of TDP-43 fibrils deposited in each type of brain (Hasegawa et al., 2008; Tsuji et al., 2012). Interestingly, band patterns of CTFs characteristic of the individual seeds were seen in intracellular TDP-43 aggregates in cultured cells, indicating that plasmid-derived TDP-43 aggregation occurs in a self-templating manner. The seeding activity of insoluble TDP-43 from patients' brains was stable against detergents, heat

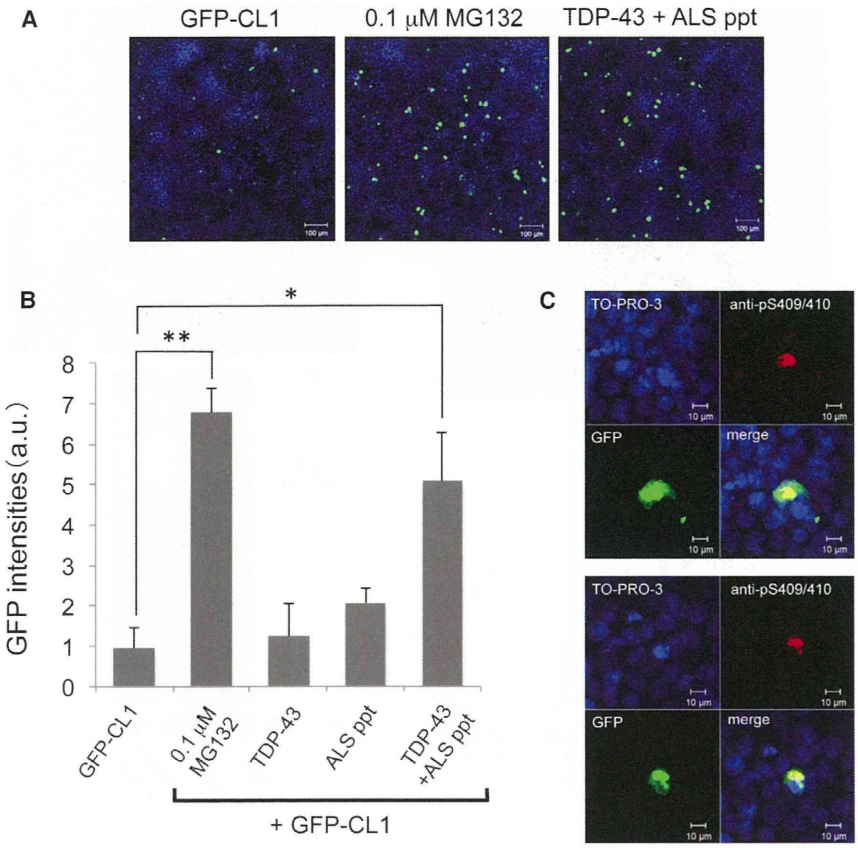

Figure 6. Proteasome Dysfunction in Cells Bearing Intracellular TDP-43 Aggregates

(A–C) SH-SY5Y cells transfected with both GFP-CL1 and TDP-43 were treated with ALS ppt for 2 days.

(A) As a control, cells expressing GFP-CL1 with or without 0.1 μM MG132 or ALS ppt, and cells expressing both GFP-CL1 and TDP-43 were also analyzed.

(B) The intensity of GFP fluorescence in these cells was quantified. The results are expressed as means + SEM (n = 3). *$p < 0.05$; **$p < 0.001$ versus the value of GFP-CL1 by Student's t test. a.u., arbitrary unit.

(C) Cells transfected with both GFP-CL1 and TDP-43 and treated with ALS ppt were stained with anti-pS409/410.

treatment, or proteolytic digestion, and cell-to-cell transmission ability was retained. Formic acid abrogated the seeding ability, suggesting that β-sheet structure in insoluble TDP-43 is indispensable for this ability. Thus, insoluble TDP-43 in the brains of patients has the characteristics of a pathogenic prion, suggesting that TDP-43 proteinopathy involves mechanisms similar to those of prion disease. It remains unclear, however, how protein aggregates spread between cells in vivo. It seems likely that prion-like aggregates are released from cells and taken up by neighboring cells, where they penetrate the cytoplasm and act as nuclei for further aggregation (Goedert et al., 2010). Prions are transferred between cultured cells via exosomes or tunneling nanotubes (Fevrier et al., 2004; Gousset et al., 2009), and our results indicate that TDP-43 aggregates may also be transferred from cell to cell at least partly via exosomes. Further investigation is needed to elucidate in detail the mechanisms of intercellular propagation of protein aggregates in vitro and in vivo. Nevertheless, taken together, our data suggest that TDP-43 proteinopathy can be classified as a prion disease.

Phosphorylated TDP-43 CTFs, as well as phosphorylated full-length TDP-43, are deposited in affected neurons in TDP-43 proteinopathy (Hasegawa et al., 2008, 2011). TDP-43 CTFs identified in FTLD-TDP brains are more prone to form aggregates than the full-length molecule in cultured cells (Igaz et al., 2009; Nonaka et al., 2009). Further, they bind with full-length TDP-43 and may facilitate aggregation of full-length TDP-43 in cultured cells (Budini et al., 2012; Nonaka et al., 2009; Zhang et al., 2009). Therefore, generation of pathogenic TDP-43 CTFs may be crucial for the formation of intracellular TDP-43 inclusions leading to neuronal cell death. However, our time-course immunoblotting analyses (Figure 2) showed that full-length TDP-43 aggregation preceded the deposition of CTFs, suggesting that cleavage of TDP-43 to produce CTFs is not a trigger for intracellular TDP-43 aggregate formation. Thus, it appears that the generation of CTFs is a consequence of degradation of phosphorylated full-length TDP-43 to eliminate abnormal and toxic aggregates of TDP-43, rather than a cause of aggregation of full-length TDP-43. In other words, TDP-43 CTFs deposited in affected neurons represent the residual stable core portion of TDP-43 aggregates left after degradation by intracellular proteolytic systems.

Abnormal posttranslational modifications and abnormal structure of seeds for aggregation are important for reproducing the pathological and biochemical features of TDP-43 inclusions found in the brains of patients with TDP-43 proteinopathy in cultured cells. Indeed, intracellular TDP-43 aggregates obtained using recombinant TDP-43 fibrils as seeds appeared as very small dot-like structures without phosphorylation (Furukawa et al., 2011), and were quite different from the TDP-43 inclusions found in the brains of patients. Our model for seeded aggregation of TDP-43 seems consistent with the pathological and biochemical changes found in the brains of patients with TDP-43 proteinopathy: in the model, aggregated TDP-43 is phosphorylated and ubiquitinated, and immunoreactivity of TDP-43 in nuclei of cells containing cytoplasmic TDP-43 aggregates is relatively weak. We also observed significant cell death and proteasome dysfunction associated with the presence of intracellular TDP-43 aggregates. It is possible that such proteasome dysfunction is caused by overloading of the ubiquitin-proteasome system with ubiquitinated proteins, including TDP-43 aggregates. The resulting suppression of proteasome activity might induce cell death. We previously observed a similar phenomenon (Nonaka et al., 2010); i.e., seed-dependent intracellular

Cell PRESS
Open ACCESS

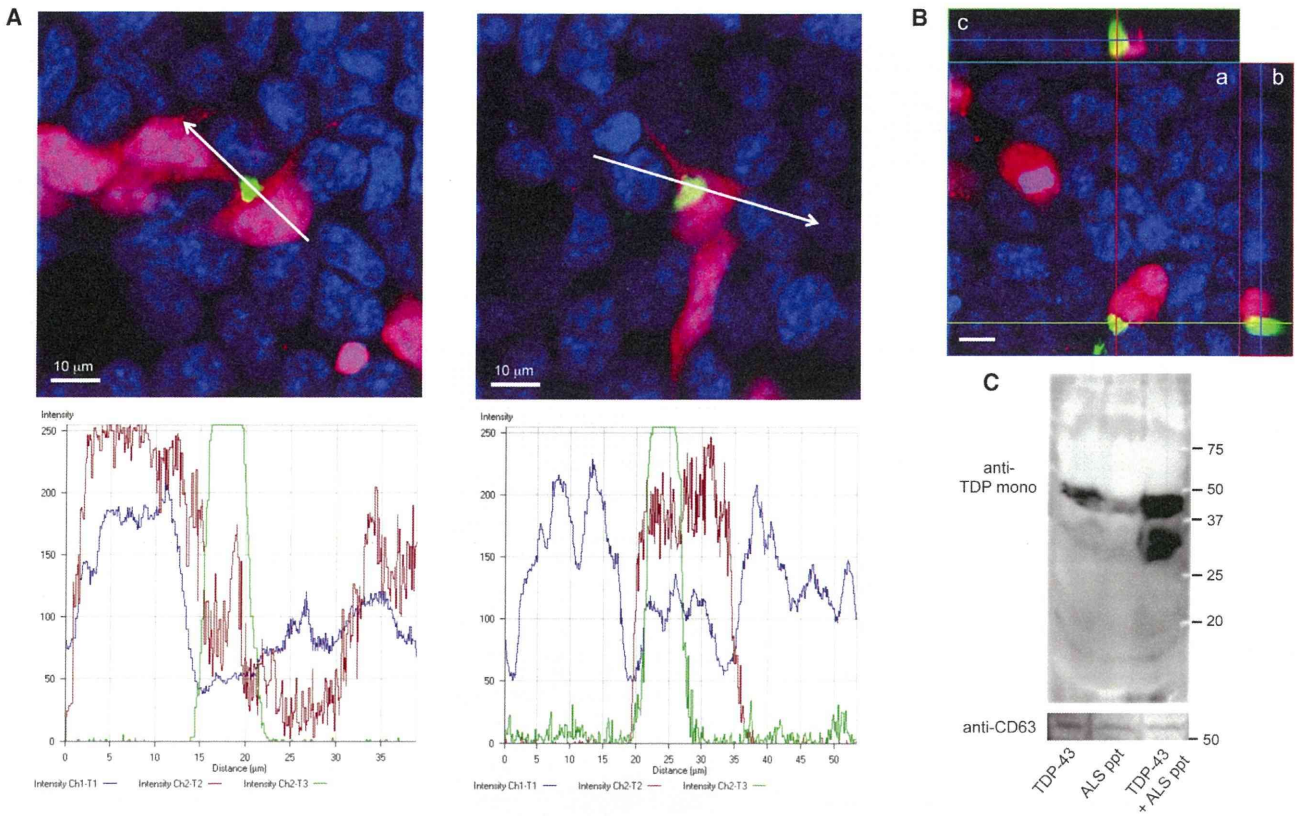

Figure 7. Intracellular TDP-43 Aggregates Are Released in Association with Exosome

(A) Coculture of cells expressing DsRed and cells having intracellular TDP-43 aggregates in a 1:1 ratio. After incubation for 3 days, cells were stained with pS409/410 (green) and counterstained with TO-PRO-3 (blue). The graphs show the intensity distribution profile of DsRed (red line), phosphorylated TDP-43 (green line), and TO-PRO-3, a nuclear marker (blue line), in the merged image. Scale bars: 10 μm.

(B) Cross-sections of reconstructed TDP-43 aggregates in these cocultured cells. (a) One of the optical sections (X-Y) at the depth indicated with blue lines in (b) and (c). (b) Cross-sectional Y-Z image along the green line indicated in (a). (c) Cross-sectional X-Z image along the red line indicated in (a). Red, DsRed; green, phosphorylated TDP-43 aggregate positive for anti-pS409/410; blue, TO-PRO-3 (nuclei). Scale bars: 10 μm.

(C) Immunoblot analyses of exosome fractions prepared from culture medium of cells expressing TDP-43 (TDP-43), cells treated with ALS ppt alone (ALS ppt), and cells expressing TDP-43 and treated with ALS ppt (TDP-43+ALS ppt). Blots were probed with anti-TDP-43 monoclonal (ProteinTech) and an antibody against CD63 (SBI).

aggregation of α-synuclein caused proteasome dysfunction and cell death.

In summary, our results show that insoluble TDP-43 in the brains of patients has prion-like features, and we consider that the onset and progression of TDP-43 proteinopathy may be associated with the propagation of TDP-43 aggregates between neuronal cells. If this is so, suppressing the propagation of aggregated proteins may be a new therapeutic strategy for many neurodegenerative diseases.

EXPERIMENTAL PROCEDURES

Preparation of Detergent-Insoluble Fractions from Brains of Patients

Human brain tissues were obtained from Fukushimura Hospital, Aichi Medical University (Aichi, Japan), Shizuoka Institute of Epilepsy and Neurological Disorders (Shizuoka, Japan), and Tokyo Metropolitan Institute of Gerontology (Tokyo, Japan). This study was approved by the local research ethics committee of Tokyo Metropolitan Institute of Medical Science (approval No. 12-3). The subjects included four patients with ALS, one with FTLD-TDP type A, three with FTLD-TDP type C, one with dementia with Lewy bodies, and one with Pick's disease. All patients with ALS met the revised El Escorial criteria for ALS (Brooks, 1994) without dementia. All patients with FTLD-TDP met the clinical diagnostic criteria of FTLD (Neary et al., 1998), and TDP-43 subtypes were classified according to published guidelines (Mackenzie et al., 2011).

Brain samples (0.5 g) from patients with ALS, FTLD-TDP, or Pick's disease were each homogenized in 2.5 ml of homogenization buffer (HB: 10 mM Tris-HCl, pH 7.5 containing 0.8 M NaCl, 1 mM EGTA, 1 mM dithiothreitol). Sarkosyl was added to the lysates (final concentration: 1%), which were then incubated for 30 min at 37°C, and centrifuged at 12,000 *g* for 10 min at room temperature. The supernatant was further centrifuged at 100,000 *g* for 10 min at room temperature. The pellet was suspended in 2 ml PBS by sonication. Lysates were divided into four tubes (each 500 μL) and centrifuged at 100,000 *g* for 20 min at room temperature. The resulting pellets were used as the detergent-insoluble fraction (ppt).

For immuno-electron microscopy analyses, the detergent-insoluble fractions prepared from brains were placed on collodion-coated, 300-mesh copper grids and stained with anti-pS409/410 and 2% (v/v) phosphotungstate. Micrographs were recorded on a JEOL JEM-1400 electron microscope.

In ID experiments, mixtures of anti-pS409/410 and anti-TDP-43 polyclonal antibody (Proteintech; 2 μl each) were added to 20 μl of ALS ppt suspension

in PBS, followed by addition of 10 μl of protein G-Sepharose (Sigma). After overnight incubation at 4°C, the supernatant was recovered. As a control, the other half of the lysate was incubated with a mixture of nonspecific mouse and rabbit immunoglobulin G (IgG; Cosmo Bio) and the same amount of protein G-Sepharose. An 8 μl aliquot of the supernatant was introduced into cells as described below.

In formic acid treatment, the detergent-insoluble fractions were suspended in 100 μl of 100% (v/v) formic acid (Nacalai Tesque) and incubated at room temperature for 30 min. After incubation, 900 μl of water was added and the mixtures were evaporated. The resulting residues were suspended in 500 μl of 0.1 M triethylammonium bicarbonate buffer (Fluka) and evaporated again. The residues were also suspended in 500 μl of water and centrifuged at 100,000 *g* for 20 min at room temperature. The resulting pellets were suspended in 100 μl of PBS and the mixtures were used for introduction experiments (see below).

Cell Culture and Transfection of Expression Plasmids

Human neuroblastoma SH-SY5Y cells obtained from ATCC were cultured in Dulbecco's modified Eagle's medium (DMEM)/F12 medium (Sigma-Aldrich) supplemented with 10% (v/v) fetal calf serum, penicillin-streptomycin-glutamine (Gibco), and MEM nonessential amino acids solution (Gibco). The cells were maintained at 37°C under a humidified atmosphere of 5% (v/v) CO_2 in air. They were grown to 50% confluence in six-well culture dishes for transient expression and then transfected with expression plasmids (usually 1 μg) using FuGENE6 (Roche) according to the manufacturer's instructions. Under our conditions, the efficiency of transfection using pEGFP-C1 vector was 20%–30%.

Introduction of Insoluble Proteins into Cells

Detergent-insoluble fractions prepared as described above were suspended in 150 μl PBS by sonication. Then 5 μg of insoluble fraction was mixed with 120 μl of Opti-MEM (Gibco), and 62.5 μl of Multifectam was added. After incubation for 30 min at room temperature, 62.5 μl of Opti-MEM was added and incubation was continued for 5 min at room temperature. Then, the mixtures were added to cells (mock cells or cells expressing HA-TDP-43, non-tagged TDP-43, or TDP-43 ΔNLS) and incubation was continued for 6 hr in a CO_2 incubator. After incubation, the medium was changed to fresh DMEM/F12 and culture was continued for the indicated period in each case. The cells were harvested and cellular proteins were differentially extracted and immunoblotted with the indicated antibodies, as previously described (Nonaka et al., 2010). Under our conditions, the efficiency of introduction of brain extracts was ~10%.

Confocal Microscopy

SH-SY5Y cells on coverslips were transfected with the indicated plasmids and cultured for 14 hr as described above. Then, the detergent-insoluble fraction was introduced and culture was continued for ~1–2 days. After fixation with 4% paraformaldehyde, cells were stained with the appropriate primary and secondary antibodies as described previously (Nonaka et al., 2010). Fluorescence was analyzed with a laser scanning confocal fluorescence microscope (LSM5 Pascal; Carl Zeiss). Confocal Z slices with an interval of 0.2 or 0.5 μm were obtained and reconstructed for three-dimensional observation using LSM5 Pascal v 4.0 software.

Cell Death Assay

Cell death assays were performed using a CytoTox 96 Non-Radioactive Cytotoxicity Assay Kit (Promega).

Assay of Proteasome Activity

In a GFP-reporter assay to monitor proteasome activity in cultured cells by confocal laser microscopy, SH-SY5Y cells that had been transfected with pcDNA3-HA-TDP-43 (1 μg) and GFP-CL1 (0.3 μg) using FuGENE6 and then treated with detergent-insoluble fraction of ALS brain were grown on coverslips for 2 days or treated with 0.1 μM MG132 overnight (Nonaka and Hasegawa, 2009; Nonaka et al., 2010). These cells were analyzed with the use of a laser-scanning confocal fluorescence microscope (LSM5Pascal; Carl Zeiss).

Coculture of Cells

SH-SY5Y cells transiently expressing DsRed (3 days after transfection) were mixed equally with cells expressing TDP-43 and treated with ALS ppt (3 days after introduction of ALS ppt). The cocultured cells were grown for a further 3 days, fixed with 4% paraformaldehyde, stained with anti-pS409/410 and TO-PRO-3, and observed under a laser-scanning confocal fluorescence microscope (LSM5Pascal; Carl Zeiss).

Preparation of Exosome Fractions

Exosome fractions were prepared from 4 ml of culture medium of cells expressing TDP-43, cells treated with ALS ppt, or cells transfected with both TDP-43 and ALS ppt, which had been cultured for 3 days after transfection, using an ExoQuick-TC kit from SBI according to the manufacturer's protocol. The exosome fractions were dissolved in 100 μl of SDS sample buffer and immunoblotted.

Statistical Analysis

Statistical analyses were performed using GraphPad Prism 4 software (GraphPad Software). Biochemical data were statistically analyzed using the unpaired, two-tailed Student's t test. A p value of ≤ 0.05 was considered to be statistically significant. For further details regarding the materials and methods used in this work, see Extended Experimental Procedures.

SUPPLEMENTAL INFORMATION

Supplemental Information includes Extended Experimental Procedures and three figures and can be found with this article online at http://dx.doi.org/10.1016/j.celrep.2013.06.007.

ACKNOWLEDGMENTS

We thank Makiko Yamashita and Masato Hosokawa for helpful comments. This work was supported by a Grant-in-Aid for Scientific Research (C) (JSPS KAKENHI 22500345 to T.N.), a Grant-in-Aid for Scientific Research (S) (JSPS KAKENHI 23228004 to M.H.) a Grant-in-Aid for Scientific Research (A) (JSPS KAKENHI 23240050 to M.H.), MHLW Grant (Number 12946221 to M.H.), a Grant-in-Aid for Scientific Research on Innovative Area "Brain Environment" (MEXT KAKENHI 24111556 to T.N.), and a grant from the Takeda Science Foundation (to T.N.).

Received: March 12, 2013
Revised: May 17, 2013
Accepted: June 6, 2013
Published: July 3, 2013

REFERENCES

Arai, T., Hasegawa, M., Akiyama, H., Ikeda, K., Nonaka, T., Mori, H., Mann, D., Tsuchiya, K., Yoshida, M., Hashizume, Y., and Oda, T. (2006). TDP-43 is a component of ubiquitin-positive tau-negative inclusions in frontotemporal lobar degeneration and amyotrophic lateral sclerosis. Biochem. Biophys. Res. Commun. *351*, 602–611.

Arai, T., Hasegawa, M., Nonoka, T., Kametani, F., Yamashita, M., Hosokawa, M., Niizato, K., Tsuchiya, K., Kobayashi, Z., Ikeda, K., et al. (2010). Phosphorylated and cleaved TDP-43 in ALS, FTLD and other neurodegenerative disorders and in cellular models of TDP-43 proteinopathy. Neuropathology *30*, 170–181.

Bence, N.F., Sampat, R.M., and Kopito, R.R. (2001). Impairment of the ubiquitin-proteasome system by protein aggregation. Science *292*, 1552–1555.

Bigio, E.H., Wu, J.Y., Deng, H.X., Bit-Ivan, E.N., Mao, Q., Ganti, R., Peterson, M., Siddique, N., Geula, C., Siddique, T., and Mesulam, M. (2013). Inclusions in frontotemporal lobar degeneration with TDP-43 proteinopathy (FTLD-TDP) and amyotrophic lateral sclerosis (ALS), but not FTLD with FUS proteinopathy (FTLD-FUS), have properties of amyloid. Acta Neuropathol. *125*, 463–465.

Braak, H., and Braak, E. (1991). Neuropathological stageing of Alzheimer-related changes. Acta Neuropathol. *82*, 239–259.

Braak, H., Del Tredici, K., Rüb, U., de Vos, R.A., Jansen Steur, E.N., and Braak, E. (2003). Staging of brain pathology related to sporadic Parkinson's disease. Neurobiol. Aging *24*, 197–211.

Brooks, B.R. (1994). El Escorial World Federation of Neurology criteria for the diagnosis of amyotrophic lateral sclerosis. Subcommittee on Motor Neuron Diseases/Amyotrophic Lateral Sclerosis of the World Federation of Neurology Research Group on Neuromuscular Diseases and the El Escorial "Clinical Limits of Amyotrophic Lateral Sclerosis" workshop contributors. J. Neurol. Sci. *124*(*Suppl*), 96–107.

Budini, M., Buratti, E., Stuani, C., Guarnaccia, C., Romano, V., De Conti, L., and Baralle, F.E. (2012). Cellular model of TAR DNA binding protein 43 (TDP-43) aggregation based on its C-terminal Q/N rich region. J. Biol. Chem. *287*, 7512–7525.

Buratti, E., and Baralle, F.E. (2009). The molecular links between TDP-43 dysfunction and neurodegeneration. Adv. Genet. *66*, 1–34.

Buratti, E., Dörk, T., Zuccato, E., Pagani, F., Romano, M., and Baralle, F.E. (2001). Nuclear factor TDP-43 and SR proteins promote in vitro and in vivo CFTR exon 9 skipping. EMBO J. *20*, 1774–1784.

Clavaguera, F., Bolmont, T., Crowther, R.A., Abramowski, D., Frank, S., Probst, A., Fraser, G., Stalder, A.K., Beibel, M., Staufenbiel, M., et al. (2009). Transmission and spreading of tauopathy in transgenic mouse brain. Nat. Cell Biol. *11*, 909–913.

de Calignon, A., Polydoro, M., Suárez-Calvet, M., William, C., Adamowicz, D.H., Kopeikina, K.J., Pitstick, R., Sahara, N., Ashe, K.H., Carlson, G.A., et al. (2012). Propagation of tau pathology in a model of early Alzheimer's disease. Neuron *73*, 685–697.

Desplats, P., Lee, H.J., Bae, E.J., Patrick, C., Rockenstein, E., Crews, L., Spencer, B., Masliah, E., and Lee, S.J. (2009). Inclusion formation and neuronal cell death through neuron-to-neuron transmission of alpha-synuclein. Proc. Natl. Acad. Sci. USA *106*, 13010–13015.

Fevrier, B., Vilette, D., Archer, F., Loew, D., Faigle, W., Vidal, M., Laude, H., and Raposo, G. (2004). Cells release prions in association with exosomes. Proc. Natl. Acad. Sci. USA *101*, 9683–9688.

Frost, B., Jacks, R.L., and Diamond, M.I. (2009). Propagation of tau misfolding from the outside to the inside of a cell. J. Biol. Chem. *284*, 12845–12852.

Furukawa, Y., Kaneko, K., Watanabe, S., Yamanaka, K., and Nukina, N. (2011). A seeding reaction recapitulates intracellular formation of Sarkosyl-insoluble transactivation response element (TAR) DNA-binding protein-43 inclusions. J. Biol. Chem. *286*, 18664–18672.

Goedert, M., Clavaguera, F., and Tolnay, M. (2010). The propagation of prion-like protein inclusions in neurodegenerative diseases. Trends Neurosci. *33*, 317–325.

Gousset, K., Schiff, E., Langevin, C., Marijanovic, Z., Caputo, A., Browman, D.T., Chenouard, N., de Chaumont, F., Martino, A., Enninga, J., et al. (2009). Prions hijack tunnelling nanotubes for intercellular spread. Nat. Cell Biol. *11*, 328–336.

Guo, W., Chen, Y., Zhou, X., Kar, A., Ray, P., Chen, X., Rao, E.J., Yang, M., Ye, H., Zhu, L., et al. (2011). An ALS-associated mutation affecting TDP-43 enhances protein aggregation, fibril formation and neurotoxicity. Nat. Struct. Mol. Biol. *18*, 822–830.

Hasegawa, M., Arai, T., Nonaka, T., Kametani, F., Yoshida, M., Hashizume, Y., Beach, T.G., Buratti, E., Baralle, F., Morita, M., et al. (2008). Phosphorylated TDP-43 in frontotemporal lobar degeneration and amyotrophic lateral sclerosis. Ann. Neurol. *64*, 60–70.

Hasegawa, M., Nonaka, T., Tsuji, H., Tamaoka, A., Yamashita, M., Kametani, F., Yoshida, M., Arai, T., and Akiyama, H. (2011). Molecular dissection of TDP-43 proteinopathies. J. Mol. Neurosci. *45*, 480–485.

Igaz, L.M., Kwong, L.K., Chen-Plotkin, A., Winton, M.J., Unger, T.L., Xu, Y., Neumann, M., Trojanowski, J.Q., and Lee, V.M. (2009). Expression of TDP-43 C-terminal fragments in vitro recapitulates pathological features of TDP-43 proteinopathies. J. Biol. Chem. *284*, 8516–8524.

Kordower, J.H., Chu, Y., Hauser, R.A., Freeman, T.B., and Olanow, C.W. (2008). Lewy body-like pathology in long-term embryonic nigral transplants in Parkinson's disease. Nat. Med. *14*, 504–506.

Li, J.Y., Englund, E., Holton, J.L., Soulet, D., Hagell, P., Lees, A.J., Lashley, T., Quinn, N.P., Rehncrona, S., Björklund, A., et al. (2008). Lewy bodies in grafted neurons in subjects with Parkinson's disease suggest host-to-graft disease propagation. Nat. Med. *14*, 501–503.

Liu, L., Drouet, V., Wu, J.W., Witter, M.P., Small, S.A., Clelland, C., and Duff, K. (2012). Trans-synaptic spread of tau pathology in vivo. PLoS ONE *7*, e31302.

Luk, K.C., Song, C., O'Brien, P., Stieber, A., Branch, J.R., Brunden, K.R., Trojanowski, J.Q., and Lee, V.M. (2009). Exogenous alpha-synuclein fibrils seed the formation of Lewy body-like intracellular inclusions in cultured cells. Proc. Natl. Acad. Sci. USA *106*, 20051–20056.

Luk, K.C., Kehm, V., Carroll, J., Zhang, B., O'Brien, P., Trojanowski, J.Q., and Lee, V.M. (2012a). Pathological α-synuclein transmission initiates Parkinson-like neurodegeneration in nontransgenic mice. Science *338*, 949–953.

Luk, K.C., Kehm, V.M., Zhang, B., O'Brien, P., Trojanowski, J.Q., and Lee, V.M. (2012b). Intracerebral inoculation of pathological α-synuclein initiates a rapidly progressive neurodegenerative α-synucleinopathy in mice. J. Exp. Med. *209*, 975–986.

Mackenzie, I.R., Neumann, M., Baborie, A., Sampathu, D.M., Du Plessis, D., Jaros, E., Perry, R.H., Trojanowski, J.Q., Mann, D.M., and Lee, V.M. (2011). A harmonized classification system for FTLD-TDP pathology. Acta Neuropathol. *122*, 111–113.

Masuda-Suzukake, M., Nonaka, T., Hosokawa, M., Oikawa, T., Arai, T., Akiyama, H., Mann, D.M.A., and Hasegawa, M. (2013). Prion-like spreading of pathological α-synuclein in brain. Brain *136*, 1128–1138.

Neary, D., Snowden, J.S., Gustafson, L., Passant, U., Stuss, D., Black, S., Freedman, M., Kertesz, A., Robert, P.H., Albert, M., et al. (1998). Frontotemporal lobar degeneration: a consensus on clinical diagnostic criteria. Neurology *51*, 1546–1554.

Neumann, M., Sampathu, D.M., Kwong, L.K., Truax, A.C., Micsenyi, M.C., Chou, T.T., Bruce, J., Schuck, T., Grossman, M., Clark, C.M., et al. (2006). Ubiquitinated TDP-43 in frontotemporal lobar degeneration and amyotrophic lateral sclerosis. Science *314*, 130–133.

Nonaka, T., and Hasegawa, M. (2009). A cellular model to monitor proteasome dysfunction by alpha-synuclein. Biochemistry *48*, 8014–8022.

Nonaka, T., Kametani, F., Arai, T., Akiyama, H., and Hasegawa, M. (2009). Truncation and pathogenic mutations facilitate the formation of intracellular aggregates of TDP-43. Hum. Mol. Genet. *18*, 3353–3364.

Nonaka, T., Watanabe, S.T., Iwatsubo, T., and Hasegawa, M. (2010). Seeded aggregation and toxicity of alpha-synuclein and tau: cellular models of neurodegenerative diseases. J. Biol. Chem. *285*, 34885–34898.

Pesiridis, G.S., Lee, V.M., and Trojanowski, J.Q. (2009). Mutations in TDP-43 link glycine-rich domain functions to amyotrophic lateral sclerosis. Hum. Mol. Genet. *18*(R2), R156–R162.

Polymenidou, M., and Cleveland, D.W. (2011). The seeds of neurodegeneration: prion-like spreading in ALS. Cell *147*, 498–508.

Ren, P.H., Lauckner, J.E., Kachirskaia, I., Heuser, J.E., Melki, R., and Kopito, R.R. (2009). Cytoplasmic penetration and persistent infection of mammalian cells by polyglutamine aggregates. Nat. Cell Biol. *11*, 219–225.

Sephton, C.F., Good, S.K., Atkin, S., Dewey, C.M., Mayer, P., 3rd, Herz, J., and Yu, G. (2010). TDP-43 is a developmentally regulated protein essential for early embryonic development. J. Biol. Chem. *285*, 6826–6834.

Snowden, J.S., Neary, D., and Mann, D.M. (2002). Frontotemporal dementia. Br. J. Psychiatry *180*, 140–143.

Tsuji, H., Arai, T., Kametani, F., Nonaka, T., Yamashita, M., Suzukake, M., Hosokawa, M., Yoshida, M., Hatsuta, H., Takao, M., et al. (2012). Molecular analysis and biochemical classification of TDP-43 proteinopathy. Brain *135*, 3380–3391.

Wu, L.S., Cheng, W.C., Hou, S.C., Yan, Y.T., Jiang, S.T., and Shen, C.K. (2010). TDP-43, a neuro-pathosignature factor, is essential for early mouse embryogenesis. Genesis *48*, 56–62.

Zhang, Y.J., Xu, Y.F., Cook, C., Gendron, T.F., Roettges, P., Link, C.D., Lin, W.L., Tong, J., Castanedes-Casey, M., Ash, P., et al. (2009). Aberrant cleavage of TDP-43 enhances aggregation and cellular toxicity. Proc. Natl. Acad. Sci. USA *106*, 7607–7612.

Journal of the Neurological Sciences 335 (2013) 89–95

Contents lists available at ScienceDirect

Journal of the Neurological Sciences

journal homepage: www.elsevier.com/locate/jns

Pathological features of FTLD-FUS in a Japanese population: Analyses of nine cases

Zen Kobayashi [a,b], Ito Kawakami [a,f], Tetsuaki Arai [a,d], Osamu Yokota [e], Kuniaki Tsuchiya [a], Hiromi Kondo [a], Yoko Shimomura [a], Chie Haga [a], Naoya Aoki [a,f], Masato Hasegawa [a], Masato Hosokawa [a], Kenichi Oshima [g], Kazuhiro Niizato [g], Hideki Ishizu [h], Seishi Terada [e], Mitsumoto Onaya [i], Manabu Ikeda [j], Kiyomitsu Oyanagi [k], Imaharu Nakano [l], Shigeo Murayama [m], Haruhiko Akiyama [a,*], Hidehiro Mizusawa [c]

[a] Tokyo Metropolitan Institute of Medical Science, Tokyo, Japan
[b] Department of Neurology, JA Toride Medical Center, Toride, Ibaraki, Japan
[c] Department of Neurology and Neurological Science, Graduate School, Tokyo Medical and Dental University, Tokyo, Japan
[d] Department of Psychiatry, Graduate School of Comprehensive Human Sciences, University of Tsukuba, Ibaraki, Japan
[e] Department of Neuropsychiatry, Okayama University Graduate School of Medicine, Dentistry and Pharmaceutical Sciences, Okayama, Japan
[f] Department of Psychiatry, Yokohama City University School of Medicine, Yokohama, Japan
[g] Tokyo Metropolitan Matsuzawa Hospital, Tokyo, Japan
[h] Department of Laboratory Medicine, Zikei Institute of Psychiatry, Okayama, Japan
[i] National Hospital Organization Shimofusa Psychiatric Medical Center, Chiba, Japan
[j] Department of Neuropsychiatry, Faculty of Life Sciences, Kumamoto University, Kumamoto, Japan
[k] Division of Neuropathology, Department of Brain Disease Research, Shinshu University School of Medicine, Nagano, Japan
[l] Tokyo Metropolitan Neurological Hospital, Fuchu, Japan
[m] Tokyo Metropolitan Geriatric Hospital & Institute of Gerontology, Tokyo, Japan

ARTICLE INFO

Article history:
Received 21 June 2013
Received in revised form 22 August 2013
Accepted 26 August 2013
Available online 4 September 2013

Keywords:
Frontotemporal lobar degeneration
Fused in sarcoma
Immunohistochemistry
BIBD
NIFID
aFTLD-U

ABSTRACT

We investigated the pathological features of frontotemporal lobar degeneration (FTLD) with fused in sarcoma protein (FUS) accumulation (FTLD-FUS) in the Japanese population. Only one out of nine FTLD-FUS cases showed pathology that corresponds to atypical FTLD with ubiquitin-positive inclusions (aFTLD-U). Five were basophilic inclusion body disease (BIBD) and two were neuronal intermediate filament inclusion disease. The last case was unclassifiable and was associated with dystrophic neurites (DNs) as the predominant FUS pathology. The results of this study indicate an ethnic difference from western countries. In Japan, BIBD is the most common subtype of FTLD-FUS and aFTLD-U is rare, a finding which contrasts with aFTLD-U being the most common form in western countries. Immunohistochemical analyses of these FTLD-FUS cases reveal that FUS abnormally accumulated in neuronal cytoplasmic inclusions (NCIs) and DNs has an immunohistochemical profile distinct from that of normal, nuclear FUS. NCIs and DNs are more readily stained than the nuclei by antibodies to the middle portion of FUS. Antibodies to the carboxyl terminal portion, on the other hand, stain the nuclei more readily than NCIs and DNs. Such an immunohistochemical profile of NCIs and DNs was similar to that of cytoplasmic granular FUS staining which we previously reported to be associated with dendrites and synapses. Redistribution of FUS from the nucleus to the cytoplasm could be associated with the formation of abnormal FUS aggregates in FTLD-FUS.

1. Introduction

Following the identification of mutations in the gene encoding the fused in sarcoma protein (FUS) as the cause of familial amyotrophic lateral sclerosis (FALS) type 6, where FUS was shown to be accumulated in motor neurons [1,2], deposition of FUS in inclusions was discovered in frontotemporal lobar degeneration (FTLD) [3] in which the inclusions are negative for tau and TAR DNA-binding protein 43 (TDP-43). A large part of FTLD with ubiquitin-positive inclusions (FTLD-U), i.e., tau negative FTLD, is FTLD with TDP-43 accumulation (FTLD-TDP), but 5–20% of FTLD-U cases are TDP-43 negative. The vast majority of such cases are now considered to be FTLD with FUS accumulation (FTLD-FUS) [4–7]. At present, neither abnormal phosphorylation nor truncation has been shown in accumulated FUS, an observation which contrasts with other abnormally accumulated proteins, such as tau, α-synuclein and TDP-43, in neurodegenerative diseases. The only reported evidence for

* Corresponding author at: Dementia Project, Tokyo Metropolitan Institute of Medical Science, 2-1-6 Kamikitazawa, Setagaya-ku, Tokyo 156-8506, Japan. Tel.: +81 3 6834 2323; fax: +81 3 5316 3150.
E-mail address: akiyama-hr@igakuken.or.jp (H. Akiyama).

0022-510X/$ – see front matter © 2013 Elsevier B.V. All rights reserved.
http://dx.doi.org/10.1016/j.jns.2013.08.035

a biochemical change of abnormally accumulated FUS is increased insolubility [3].

FTLD-FUS is considered to consist of three pathological subtypes, atypical FTLD-U (aFTLD-U), basophilic inclusion body disease (BIBD) and neuronal intermediate filament inclusion disease (NIFID) [3,5,8–12]. Of these three subtypes, aFTLD-U is characterized neuropathologically by the occurrence of neuronal cytoplasmic inclusions (NCIs) positive for ubiquitin but mostly invisible by hematoxylin and eosin (HE) staining. In western countries, aFTLD-U is the most common subtype of FTLD-FUS [12–14]. NIFID is characterized by NCIs that contain class IV neuronal intermediate filaments [15–18]. NCIs in this subtype sometimes have HE-unstained central compartments [15] or eosinophilic cores [11,15,17,19]. In BIBD, some, but not all, NCIs are recognized as lightly basophilic inclusions by HE staining. While these three subtypes may represent a continuous spectrum of diseases [10], recent detailed histopathological comparison has suggested that they are closely related but distinct entities [5]. Basophilic inclusions are also found in FALS type 6, but BIBD as a subtype of FTLD-FUS is now clearly distinguished in that it is a sporadic disease without FUS gene mutations and the inclusions are, similarly to those in aFTLD-U and NIFID, positive for other members of the FET protein family, Ewing's sarcoma and TATA-binding protein-associated factor 15 [20,21].

In Japan, a number of differences from western countries have been recognized in the occurrence of diseases in the FTLD categories. While the majority of FTLD in western countries shows frontotemporal dementia (FTD), which is often referred to as a behavioral variant of FTD (bvFTD), semantic dementia accounts for a significant portion of FTLD in Japan [22]. From a genetic point of view, the incidence of familial FTLD is much lower in Japan than those reported in western countries [23]. Further, most familial FTLD in Japan is associated with tau mutations and FTLD with granulin mutations or C9orf72 repeat expansion is rare [24]. Considering these ethnic differences, we have reviewed all FTLD cases archived in the brain collection in the Tokyo Institute of Psychiatry, including some cases shared under collaboration with other laboratories and other cases autopsied in the Tokyo Metropolitan Matsuzawa hospital. Of 66 FTLD cases, we have found nine FTLD-FUS cases, of which only one shows pathology consistent with aFTLD-U. We have also found a characteristic immunohistochemical profile of abnormally accumulated FUS using a panel of anti-FUS antibodies that recognize different portions of the FUS molecule.

2. Materials and methods

2.1. Neuropathological examination

Brain and spinal cord tissue samples were fixed postmortem with 10% formalin and embedded in paraffin. Ten micrometer thick sections were prepared from the cerebrum, midbrain, pons, medulla oblongata, cerebellum and spinal cord. Sections were examined initially with HE, Klüver–Barrera (KB), Bodian's silver, methenamine silver and Gallyas–Blaak staining. Severity of the central nervous system (CNS) lesions was evaluated semiquantitatively using the grading system employed in a previous study [19].

2.2. Immunohistochemical staining

For immunostaining, deparaffinized sections were incubated with 1% H_2O_2 in methanol for 30 min to eliminate endogenous peroxidase activity in the tissue. Sections were pretreated by autoclaving for 10 min in 10 mM sodium citrate buffer, pH 6.0, at 120 °C. After washing three times with 0.01 M phosphate buffered saline (PBS), pH 7.4, sections were blocked with 10% normal serum from the appropriate animal species. Sections were then incubated overnight at 4 °C with one of the primary antibodies in PBS containing 0.3% Triton X-100 (PBS-Tx). After washing three times in PBS-Tx, sections were incubated in biotinylated anti-mouse or anti-rabbit secondary antibody for 1 h, and then in avidin-biotinylated horseradish peroxidase complex (ABC Elite kit, Vector) for 1 h. Peroxidase labeling was visualized with 0.2% 3,3′-diaminobenzidine (DAB) as a chromogen. Sections were counterstained with hematoxylin.

The antibodies employed for immunohistochemistry are listed in Table 1. For α-internexin staining, dilution of the antibody was chosen for each case so that we obtained weak axonal and neuronal cytoplasmic staining as an internal positive control. α-Internexin staining in 6 out of 9 cases was published previously with a different antibody (ab32306, rabbit, polyclonal, 1:100, Abcam plc) [19], and the results were consistent between the two studies.

As reported previously [3,11], sensitivity of FUS immunostaining varied among cases, presumably because of the diverse fixation conditions. Therefore, the dilution of the primary antibody was adjusted to obtain FUS immunoreactivity of neuronal nuclei in each case. Sometimes, positive staining of NCIs but not nuclei, or vice versa, was obtained even at the highest concentration of the antibody, where the non-specific background was about to blur specific labeling. To overcome such uncertainty, we used 6 anti-FUS antibodies raised against 5 different portions of the FUS molecule (Table 1).

2.3. Cases

From 1973 to 2011, the period between the foundation and closure of the Tokyo Institute of Psychiatry, 66 FTLD cases were registered in the neuropathology department of the institute. All cases fulfilled the clinical and pathological diagnostic criteria for FTLD. Of the 66 cases, 9 were FTLD-FUS. Distinctions between FTLD-FUS subtypes are based on the documentation in the literature [3,5,6,10–12]. Briefly, the diagnosis of BIBD was made when a significant number of basophilic or lightly-basophilic NCIs were found in HE staining. It is sometimes difficult to distinguish the NCIs in BIBD from those in NIFID in HE-stained sections [19]. Thus, the diagnosis of NIFID eventually relied on the result of α-internexin immunohistochemistry, where a significant number of NCIs in the neocortex were positive for α-internexin in NIFID cases. Occasional neuronal intranuclear inclusions (NIIs) also suggested that a case was unlikely to be BIBD [5,9,10]. In case 8, most NCIs were invisible in HE-stained sections and were negative for α-internexin. Together with relatively frequent NIIs in the hippocampus compared with other cases in our series, we considered this case to be aFTLD-U.

3. Results

The basic clinical information and pathological subtypes of the 9 FTLD-FUS cases are summarized in Table 2. No case had a family history of similar disorders or amyotrophic lateral sclerosis. The mean age at

Table 1
Antibodies used for immunohistochemistry.

Antibody	Type	Company	Concentration[a]
Anti-ubiquitin	Rabbit polyclonal	Dako	0.77 μg/ml
Anti-TDP43	Rabbit polyclonal	Proteintech Group	0.53 μg/ml
Anti-α-internexin (2E3)	Mouse monoclonal	Santa Cruz Biotechnology	1:100
Anti-FUS			
FUS [1–50]	Rabbit polyclonal	Abcam	1:10 to 1:100
FUS [1–50]	Rabbit polyclonal	Bethyl Laboratories	3.3–10 μg/ml
FUS [52–400]	Rabbit polyclonal	Proteintech Group	13 μg/ml
FUS [86–213]	Rabbit polyclonal	Sigma-Aldrich	0.63–6.3 μg/ml
FUS [250–300]	Rabbit polyclonal	Abcam	10–50 μg/ml
FUS [400–450]	Rabbit polyclonal	Bethyl Laboratories	50 μg/ml
FUS [500–526]	Rabbit polyclonal	Bethyl Laboratories	10–100 μg/ml

[a] When the concentration of antibody was not available in the data sheet, dilution from the original solution provided by the distributor was shown. The numbers in [] indicate amino acid sequences of the antigen to which the antibodies were raised.